

Chapter 2

The DSL in NIPI Structures of Non-Parabolic Semiconductors

2.1 Introduction

In this chapter in [Sect. 2.2.1](#), of the theoretical background, the DSL in NIPI structures of non-linear optical materials has been investigated. The [Sect. 2.2.2](#) contains the results for NIPI structures of III–V, ternary and quaternary compounds in accordance with the three and the two band models of Kane together with parabolic energy bands and they form the special cases of [Sect. 2.2.1](#). The [Sects. 2.2.3, 2.2.4](#) and [2.2.5](#) contain the study of the DSL for NIPI's of II–VI, IV–VI and stressed Kane type semiconductors respectively. The [Sects. 2.3](#) and [2.4](#) contain the results and discussion and the open research problems for this chapter.

2.2 Theoretical Background

2.2.1 Formulation of the DSL in NIPI Structures of Non-Linear Optical Materials

The dispersion relation of the conduction electrons in NIPI structures of nonlinear optical materials can be expressed by using [\(1.2\)](#) and following the method as given in [\[1, 2\]](#) as

$$\psi_1(E) = \psi_2(E)k_s^2 + \psi_3(E) \left(n_i + \frac{1}{2} \right) \frac{2m^*}{\hbar} \omega_8(E) \quad (2.1)$$

where $\omega_8(E) \equiv \left(\frac{n_0 |e|^2}{d_0 \epsilon_{sc} [\theta_1(E)]} \right)^{\frac{1}{2}}$, $\theta_1(E) \equiv \frac{\hbar}{2} \left\{ \frac{\psi_3(E)[\psi_1(E)]' - \psi_1(E)[\psi_3(E)]'}{[\psi_3(E)]^2} \right\}$, n_0 denotes the surface electron concentration per unit area for this chapter, d_0 is the super-lattice period and n_i ($= 0, 1, 2, \dots$) is the miniband index for NIPI structures.

The subband energy (E_{1ni}) can be written as

$$\psi_1(E_{1ni}) = \psi_3(E_{1ni}) \left(n_i + \frac{1}{2} \right) \frac{2m_{\parallel}^*}{\hbar} \omega_8(E_{1ni}) \quad (2.2)$$

The density-of-states function for NIPI structures of non-linear optical materials can be expressed as

$$N_{NIPI}(E) = \frac{g_v}{2\pi} \sum_{n_i=0}^{n_{\max}} R_{81}(E, n_i) H(E - E_{1ni}) \quad (2.3)$$

where $R_{81}(E, n_i) = [T'_{81}(E, n_i)]$ and $T_{81}(E, n_i) = [\psi_1(E) - \psi_3(E)(n_i + \frac{1}{2}) \frac{2m_{\parallel}^*}{\hbar} \omega_8(E)] [\psi_2(E)]^{-1}$

The electron concentration, can be written as

$$n_0 = \frac{g_v}{2\pi} \sum_{n_i=0}^{n_{\max}} \left[T_{81}(\bar{E}_{Fn}, n_i) + T_{82}(\bar{E}_{Fn}, n_i) \right] \quad (2.4)$$

where \bar{E}_{Fn} is the fermi energy in the present case, $T_{81}(\bar{E}_{Fn}, n_i) \equiv [\psi_1(\bar{E}_{Fn}) - \psi_3(\bar{E}_{Fn})(n_i + \frac{1}{2}) \frac{2m_{\parallel}^*}{\hbar} \omega_8(\bar{E}_{Fn})] [\psi_2(\bar{E}_{Fn})]^{-1}$ and $T_{82}(\bar{E}_{Fn}, n_i) \equiv \sum_{r=1}^s L(r) T_{81}(\bar{E}_{Fn}, n_i)$.

The 2D DSL in the electric quantum limit in this case is given by

$$L_{2D} = \left[\frac{e^2}{2\epsilon_{sc}} \frac{\partial n_{00}}{\partial (\bar{E}_{F0} - E_{1n0})} \right]^{-1} \quad (2.5)$$

where n_{00} , \bar{E}_{F0} and E_{1n0} are the surface electron concentration per unit area, Fermi energy and sub-band energy at the electric quantize limit respectively.

Using (2.4) at the electric quantum limit and under the condition of extreme degeneracy together with (2.5) we can investigate L_{2D} .

2.2.2 DSL in the NIPI Structures of III-V, Ternary and Quaternary Semiconductors

- (a) The electron energy spectrum in NIPI structures of III-V, ternary and quaternary materials can be expressed from (2.1) under the conditions $\Delta_{\parallel} = \Delta_{\perp} = \Delta$, $\delta = 0$ and $m_{\parallel}^* = m_{\perp}^* = m_c$, as

$$I_{11}(E) = \left(n_i + \frac{1}{2} \right) \hbar \omega_9(E) + \frac{\hbar^2 k_s^2}{2m_c} \quad (2.6)$$

where

$$\omega_9(E) \equiv \left(\frac{n_0 |e|^2}{\varepsilon_{sc} I'_{11}(E) m_c d_0} \right)^{\frac{1}{2}}. \quad (2.7)$$

The sub-band energies (E_{2ni}) can be written as

$$I_{11}(E_{2ni}) = \left(n_i + \frac{1}{2} \right) \hbar \omega_9(E_{2ni}) \quad (2.8)$$

The density-of-states function in this case can be expressed as

$$N_{NIP1}(E) = \frac{m_c g_v}{\pi \hbar^2} \sum_{n_i=0}^{n_{\max}} R_{82}(E, n_i) H(E - E_{2ni}) \quad (2.9)$$

where $R_{82}(E, n_i) = [T'_{83}(E, n_i)]$ and $[T_{83}(E, n_i)] \equiv \{ [I(E)] - (n_i + \frac{1}{2}) \hbar [\omega_9(E)] \}$

The use of (2.9) leads to the expression of the electron concentration as

$$n_0 = \frac{m_c g_v}{2\pi} \sum_{n_i=0}^{n_{\max}} [T_{83}(\bar{E}_{Fn}, n_i) + T_{84}(\bar{E}_{Fn}, n_i)] \quad (2.10)$$

where $T_{83}(\bar{E}_{Fn}, n_i) \equiv [I_{11}(\bar{E}_{Fn}) - (n_i + \frac{1}{2}) \hbar \omega_9(\bar{E}_{Fn})]$ and $T_{84}(\bar{E}_{Fn}, n_i) \equiv \sum_{r=1}^s L(r) T_{83}(\bar{E}_{Fn}, n_i)$.

Using (2.10) at the electric quantum limit and under the condition of extreme degeneracy together with (2.5), we can investigate L_{2D} .

- (b) For the two band model of Kane, the expressions of the dispersion relation, the DSL, the sub-band energies, the density-of-states function and n_0 remain same where

$$I_{11}(E) = E(1 + \alpha E), \{I_{11}(E)\}' = (1 + 2\alpha E) \text{ and } \{I_{11}(E)\}'' = 2\alpha.$$

Using (2.10) at the electric quantum limit, the condition of extreme degeneracy and the said substitutions together with (2.5), we can study DSL in this case.

- (c) For parabolic energy bands, the forms of the expressions of dispersion relation, the DSL, the sub-band energies, the density-of-states function and n_0 remain same, where $I_{11}(E) = E$, $\{I_{11}(E)\}' = 1$ and $\{I_{11}(E)\}'' = 0$.

Thus, we observe that the DSL in this case is a constant quantity as written in the preface under the conditions of extreme carrier degeneracy and electric quantum limit respectively.

2.2.3 DSL in the NIP1 Structures of II–VI Semiconductors

The carrier dispersion law in NIP1 structures of II–VI compounds can be expressed as

$$E = a'_0 k_s^2 + \left(n_i + \frac{1}{2}\right) \hbar \omega_{10} \pm \bar{\lambda}_0 k_s, \quad \omega_{10}(E) \equiv \left(\frac{n_0 |e|^2}{d_0 \epsilon_{sc} m_{\parallel}^*}\right)^{\frac{1}{2}} \quad (2.11)$$

The sub-band energies (E_{3ni}) can be written as

$$E_{3ni} = \left(n_i + \frac{1}{2}\right) \hbar \omega_{10} \quad (2.12)$$

The density-of-states function in this case can be expressed as

$$N_{NIPI}(E) = \frac{m_{\perp}^* g_v}{\pi \hbar^2} \sum_{n_i=0}^{n_{i\max}} \left[1 - \frac{a_{81}}{\sqrt{E + b_{81}(n_i)}} \right] H(E - E_{3ni}) \quad (2.13)$$

in which, $a_{81} \equiv \frac{\lambda_0}{2\sqrt{a'_0}}$ and $b_{81}(n_i) \equiv \left[\frac{1}{4a'_0} \left[(\bar{\lambda}_0)^2 - 4a'_0 \left(n_i + \frac{1}{2}\right) \hbar \omega_{10}\right]\right]$.

The use of the (2.13) leads to the electron concentration under the condition of extreme degeneracy as

$$n_{2D} = \frac{g_v m_{\perp}^*}{\pi \hbar^2} \sum_{n_i=0}^{n_{i\max}} \left(E_{Fn} - E_{3ni} + (\bar{\lambda}_0)^2 m_{\perp}^* \hbar^{-2} \right) \quad (2.14a)$$

By using (2.5) and (2.14a) at the electric quantum limit, we obtain the expression of 2D DSL as

$$L_{2D} = [(2\epsilon_{sc} \pi \hbar^2) / (e^2 m_{\perp}^* g_v)] \quad (2.14b)$$

2.2.4 DSL in the NIPI Structures of IV–VI Semiconductors

The carrier energy spectrum in NIPI structures of IV–VI compounds can be written as

$$k_s^2 = (\hbar^2 S_{19})^{-1} \left[-S_{20}(E, n_i) + \sqrt{S_{20}^2(E, n_i) + 4S_{19}S_{21}(E, n_i)} \right] \quad (2.15)$$

in which, $S_{19} \equiv \left(\frac{\alpha}{m_i^+ m_i^-}\right)$, $S_{20}(E, n_i) \equiv \left\{ \frac{1}{m_i^-} - \left(\frac{\alpha E}{m_i^+}\right) + \frac{1+\alpha E}{m_i^-} + \frac{\alpha \hbar^2}{2m_i^+ m_i^-} \left(n_i + \frac{1}{2}\right) T(E) + \frac{\alpha \hbar^2}{2m_i^- m_i^+} \left(n_i + \frac{1}{2}\right) T(E) \right\}$

$$T(E) \equiv \frac{2m^*(0)}{\hbar} \omega_{11}(E), m^*(0) \equiv \left(\frac{m_i^+ m_i^-}{m_i^* + m_i^-}\right), \omega_{11}(E) \equiv \left(\frac{n_0 |e|^2}{d_0 \epsilon_{sc} m^*(E)}\right)^{\frac{1}{2}},$$

$$\begin{aligned}
m^*(E) &\equiv \frac{1}{4t_1} \left[-(t_2(E))' + \frac{t_2(E)(t_2(E))' + 2t_1(1 + 2\alpha E)}{\sqrt{t_2^2(E) + 4Et_1(1 + \alpha E)}} \right], \\
t_1 &\equiv \left(\frac{\alpha}{4m_l^+ m_l^-} \right), t_2(E) \equiv \frac{1}{2} \left[\left(\frac{1}{m_l^*} \right) - \left(\frac{\alpha E}{m_l^+} \right) + \left(\frac{1 + \alpha E}{m_l^-} \right) \right], \\
(t_2(E))' &\equiv \frac{\alpha}{2} \left(\frac{1}{m_l^-} - \left(\frac{1}{m_l^+} \right) \right) \text{ and} \\
S_{21}(E, n_i) &\equiv \left[E(1 + \alpha E) + \frac{\alpha E \hbar^2}{2m_l^+} \left(n_i + \frac{1}{2} \right) T(E) \right. \\
&\quad + \frac{\hbar^2}{2m_l^-} \left(n_i + \frac{1}{2} \right) T(E)(1 + \alpha E) + \frac{\hbar^4}{4m_l^- m_l^+} \left(n_i + \frac{1}{2} \right) T(E) \\
&\quad \left. - \left(\frac{\hbar^2}{2m_l^*} \right) T(E) \left(n_i + \frac{1}{2} \right) \right].
\end{aligned}$$

The subband energies (E_{4ni}) can be written as

$$\begin{aligned}
&\left[E_{4ni} - \frac{\hbar^2}{2m_l^-} T(E_{4ni}) \left(n_i + \frac{1}{2} \right) \right] \left[1 + \alpha E_{4ni} + \alpha \frac{\hbar^2}{2m_l^+} T(E_{4ni}) \left(n_i + \frac{1}{2} \right) \right] \\
&= \left[\frac{\hbar^2}{2m_l^*} T(E_{4ni}) \left(n_i + \frac{1}{2} \right) \right] \quad (2.16)
\end{aligned}$$

The density-of-states function in this case assumes the form as

$$N_{nipi}(E) = \frac{g_v}{\pi \hbar^2} \sum_{n_i=0}^{n_{i\max}} R_{84}(E, n_i) H(E - E_{4ni}) \quad (2.17)$$

where $R_{84}(E, n_i) = [T'_{85}(E, n_i)]$ and $[T_{85}(E, n_i)] = [-S_{20}(E, n_i) + \sqrt{S_{20}^2(E, n_i) + 4S_{19}S_{21}(E, n_i)}]$

The use of (2.17) leads to the expression of the electron concentration as

$$n_0 = \frac{g_v}{2\pi \hbar^2 S_{19}} \sum_{n_i=0}^{n_{i\max}} [T_{85}(\bar{E}_{Fn}, n_i) + T_{86}(\bar{E}_{Fn}, n_i)] \quad (2.18)$$

where, $T_{85}(\bar{E}_{Fn}, n_i) \equiv [-S_{20}(E_{Fn}, n_i) + \sqrt{[S_{20}(E_{Fn}, n_i)]^2 + 4S_{19}S_{21}(E_{Fn}, n_i)}]$ and $T_{86}(\bar{E}_{Fn}, n_i) \equiv \sum_{r=1}^S L(r) T_{85}(\bar{E}_{Fn}, n_i)$.

Using (2.18) at the electric quantum limit and under the condition of extreme degeneracy together with (2.5), we can investigate L_{2D} .

2.2.5 DSL in the NIPI Structures of Stressed Semiconductors

The electron dispersion law in the NIPI structures of stressed semiconductors can be written as

$$\frac{k_x^2}{[\bar{a}_0(E)]^2} + \frac{k_y^2}{[\bar{b}_0(E)]^2} + \frac{1}{[\bar{c}_0(E)]^2} \frac{2m_z^*(0)}{\hbar} \left(n_i + \frac{1}{2} \right) \omega_{12}(E) = 1 \quad (2.19)$$

where $\omega_{12}(E) \equiv \left(\frac{n_0 |e|^2}{d_0 \epsilon_{sc} m_z^*(E)} \right)^{\frac{1}{2}}$ and $m_z^*(E) \equiv \hbar^2 \bar{c}_0(E) \frac{\partial}{\partial E} [\bar{c}_0(E)]$.

The subband energies (E_{5ni}) can be written as

$$\frac{1}{[\bar{c}_0(E_{4ni})]^2} \frac{2m_z^*(0)}{\hbar} \left(n_i + \frac{1}{2} \right) \omega_{12}(E_{4ni}) = 1 \quad (2.20)$$

The density-of-states function can be expressed as

$$N_{nipi}(E) = \frac{g_v}{\pi \hbar^2} \sum_{n_i=0}^{n_{\max}} R_{85}(E, n_i) H(E - E_{5ni}) \quad (2.21)$$

where $R_{85}(E, n_i) = [C_3'(E, n_i)]$ and $C_3(E, n_i) \equiv \bar{a}_0(E) \bar{b}_0(E) \left[1 - \frac{2m_z^*(0)}{\hbar} \left(n_i + \frac{1}{2} \right) \frac{\omega_{12}(E)}{(\bar{c}_0(E))^2} \right]$

Thus, using (2.21), the electron concentration in NIPI structures of stressed compounds can be written as

$$n_0 = \frac{g_v}{2\pi} \sum_{n_i=0}^{n_{\max}} \left[C_3(\bar{E}_{Fn}, n_i) + C_4(\bar{E}_{Fn}, n_i) \right] \quad (2.22)$$

where $C_3(\bar{E}_{Fn}, n_i) \equiv \bar{a}_0(\bar{E}_{Fn}) \bar{b}_0(E_{Fn}) \left[1 - \frac{2m_z^*(0)}{\hbar} \left(n_i + \frac{1}{2} \right) \frac{\omega_{12}(\bar{E}_{Fn})}{(\bar{c}_0(\bar{E}_{Fn}))^2} \right]$ and $C_4(\bar{E}_{Fn}, n_i) \equiv \sum_{r=1}^s L(r) C_3(\bar{E}_{Fn}, n_i)$

Using (2.22) at the electric quantum limit and under the condition of extreme degeneracy together with (2.5), we can investigate L_{2D} .

2.3 Results and Discussion

Using the appropriate equations with the energy band constants as given in Table 1.1, the normalized inverse DSL in the quantum limit has been plotted for the NIPI structures of Cd_3As_2 as a function of electron concentration as shown in curve (a) of Fig. 2.1. The curve (b) corresponds to $\delta = 0$ and the curve (c) exhibits the dependence of the inverse DSL on n_0 in accordance with the three-band model of Kane, respectively. The plots (d) and (e) correspond to the two-band model of Kane and that of parabolic energy bands. By comparing the curves (a) and (b) of

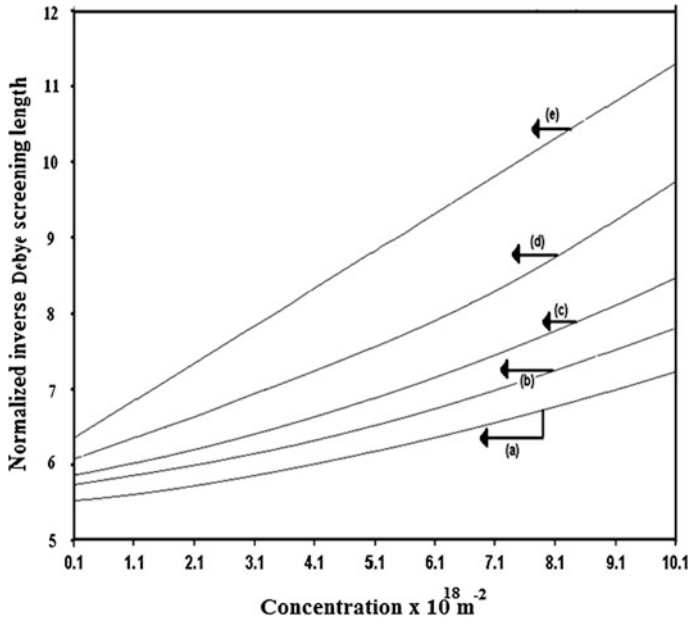


Fig. 2.1 The plot of the normalized inverse DSL in the quantum limit for NIPI structures of Cd_3As_2 as a function of electron concentration in accordance with (a) the generalized band model, (b) $\delta = 0$, (c) the three band model of Kane, (d) the two band model of Kane and (e) the parabolic energy bands

Fig. 2.1, one can assess the influence of crystal field splitting on the inverse DSL in NIPI structures of Cd_3As_2 . The Fig. 2.2 represents all cases of Fig. 2.1 for NIPI structures of CdGeAs_2 as an example. It appears from Figs. 2.1 and 2.2 that, the inverse DSL in NIPI structures of tetragonal non-linear optical materials increases with increasing carrier degeneracy as expected for degenerate materials.

Using the appropriate equations one can numerically evaluate the inverse DSL in the quantum limit as a function of electron concentration in NIPI structures of III–V compounds by using the NIPI structures of InAs, and InSb as shown in Figs. 2.3 and 2.4 by curves (a), (b) and (c) respectively, in accordance with three and two band models of Kane together with the model of parabolic energy bands.

Taking NIPI structures of $\text{Hg}_{1-x}\text{Cd}_x\text{Te}$ as an example of ternary compounds, the inverse DSL has been plotted for both the structures as a function of electron concentration as shown in Fig. 2.5 for all cases of the Fig. 2.3. It appears from the Fig. 2.5 that the inverse DSL in the quantum limit in both cases of NIPI structures of ternary compounds increases with increasing electron concentration. Taking NIPI structures of $\text{In}_{1-x}\text{Ga}_x\text{As}_y\text{P}_{1-y}$ lattice matched to InP as an example of quaternary compounds the inverse DSL in the quantum limit has been further been plotted as a function of electron concentration as shown in Fig. 2.6 in accordance with the three and two band models of Kane together with the isotropic parabolic energy band model for both the cases.

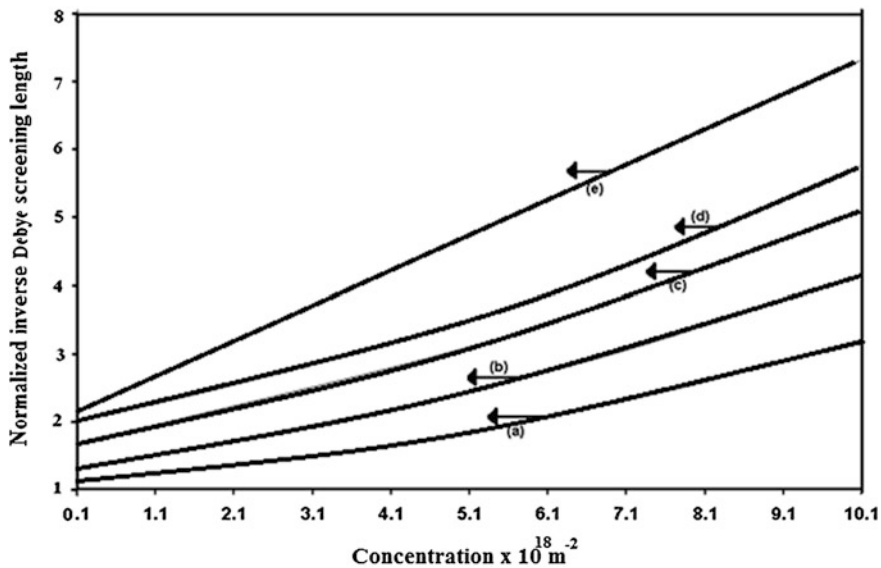


Fig. 2.2 The plot of the normalized inverse DSL in the quantum limit for NIPI structures of CdGeAs₂ as a function of electron concentration in accordance with (a) the generalized band model, (b) $\delta = 0$, (c) the three band model of Kane, (d) the two band model of Kane and (e) the parabolic energy bands

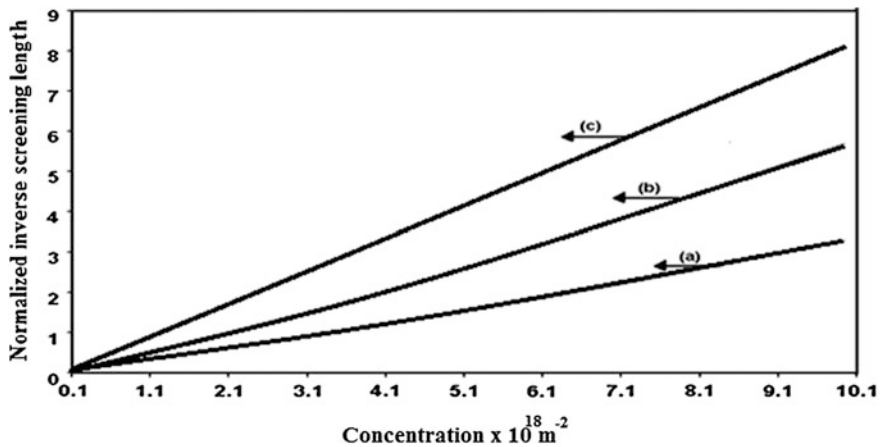


Fig. 2.3 The plot of the normalized inverse DSL in the quantum limit for NIPI structures of InAs as a function of electron concentration in accordance with (a) the three band model of Kane, (b) the two band model of Kane and (c) the parabolic energy bands

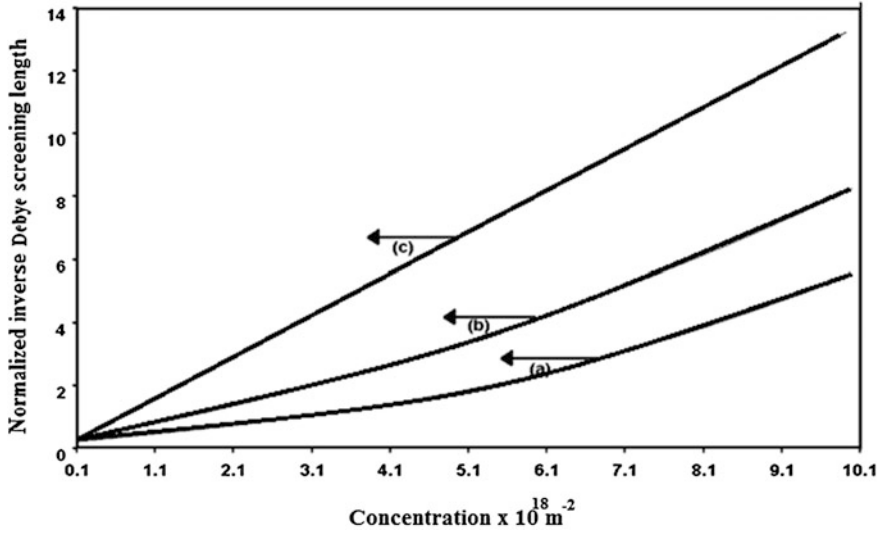


Fig. 2.4 The plot of the normalized inverse DSL in the quantum limit for NIPI structures of InSb as a function of electron concentration in accordance with (a) the three band model of Kane, (b) the two band model of Kane and (c) the parabolic energy bands

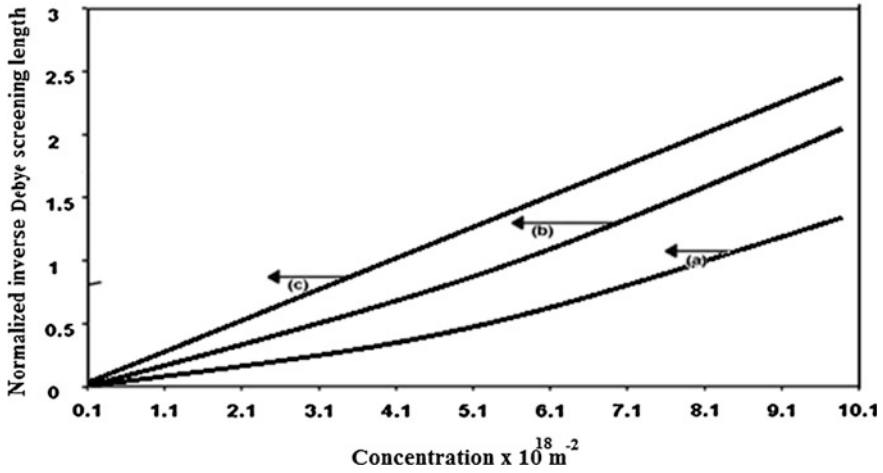


Fig. 2.5 The plot of the normalized inverse DSL in the quantum limit for NIPI structures of $\text{Hg}_{1-x}\text{Cd}_x\text{Te}$ as a function of electron concentration in accordance with (a) the three band model of Kane, (b) the two band model of Kane and (c) the parabolic energy bands

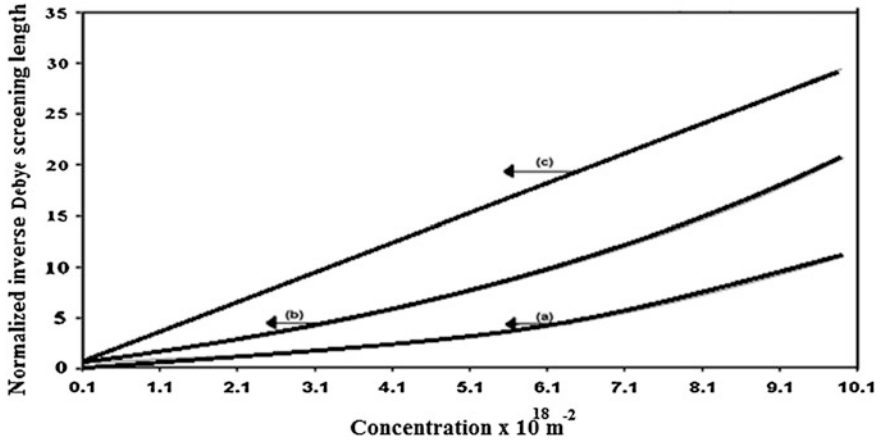


Fig. 2.6 The plot of the normalized inverse DSL in the quantum limit for NIPI structures of $\text{In}_{1-x}\text{Ga}_x\text{As}_y\text{P}_{1-y}$ lattice matched to InP as a function of electron concentration in accordance with (a) the three band model of Kane, (b) the two band model of Kane and (c) the parabolic energy bands

It appears that the inverse DSL increases with increasing n_0 and from Figs. 2.5 and 2.6, one can assess the influence of energy band constants on the inverse normalized DSL for NIPI structures of ternary and quaternary materials respectively. Using appropriate equations, the inverse DSL in the quantum limit has been plotted for the NIPI structures of CdS, as a function of carrier concentration as shown by curves (a) and (b) in Fig. 2.7 for both $\bar{\lambda}_0 \neq 0$ and $\bar{\lambda}_0 = 0$ respectively. This has been presented for the purpose of assessing the influence of the splitting of the two spin states by the spin-orbit coupling and the crystalline field on the inverse DSL for NIPI structures of II–VI materials. Using appropriate equations, in Fig. 2.8, the inverse DSL in the quantum limit has been plotted for the NIPI structures of (a) PbTe, (b) PbSnTe and (c) $\text{Pb}_{1-x}\text{Sn}_x\text{Se}$ as a function of electron concentration in accordance with the Dimmock model. For relatively low values of electron concentration, the values of the inverse DSL for the three materials exhibit convergence behavior whereas for relatively large values of n_0 , the numerical values differ widely from each other in this case. Using the appropriate equations, in Fig. 2.9, the inverse DSL in the quantum limit has been plotted for the NIPI structures of stressed InSb as a function of electron concentration. The plot (a) of Fig. 2.9 exhibits the inverse DSL in the presence of the stress while the plot (b) shows the same in the absence of the stress.

In the presence of the stress, the magnitude of the inverse DSL is being increased as compared with the same under stress free condition.

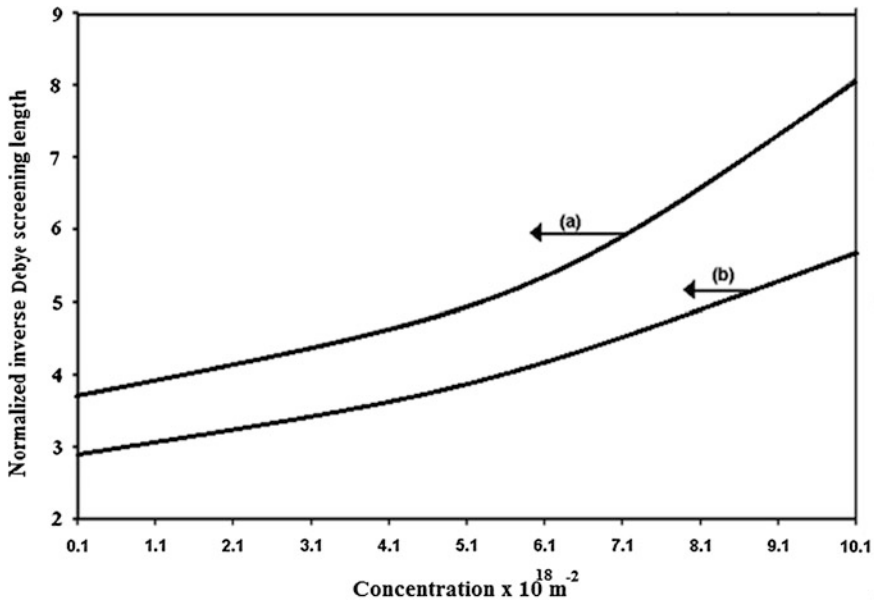


Fig. 2.7 The plot of the normalized inverse DSL in the quantum limit for NIPI structures of CdS as a function of carrier concentration in accordance with (a) $\bar{\lambda}_0 \neq 0$ and (b) $\bar{\lambda}_0 = 0$

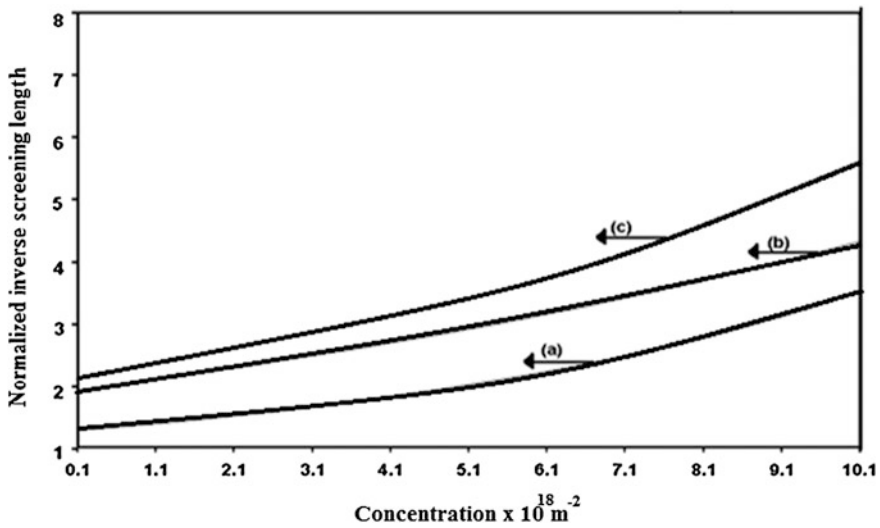


Fig. 2.8 The plot of the normalized inverse DSL in the quantum limit as a function of electron concentration for the NIPI structures of (a) PbTe, (b) PbSnTe and (c) $\text{Pb}_{1-x}\text{Sn}_x\text{Se}$

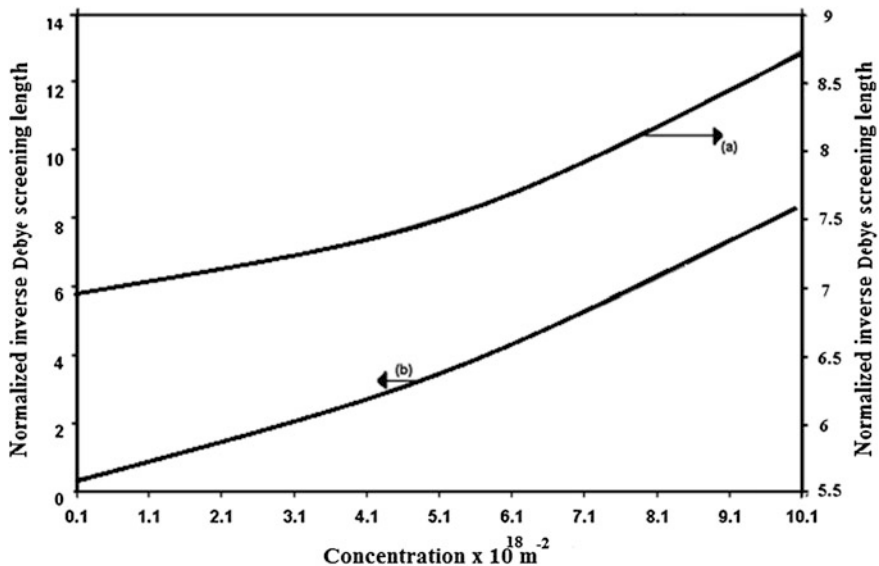


Fig. 2.9 The plot of the inverse DSL in the quantum limit as a function of electron concentration for the NIPI structures of stressed InSb in which the curve (a) is in the presence of stress and curve (b) is under absence of stress

2.4 Open Research Problems

- (R.2.1) Investigate the DSL in the presence of an arbitrarily oriented non-quantizing magnetic field for NIPI structures of non-linear optical semiconductors by including the electron spin. Study all the special cases for III–V, ternary and quaternary materials in this context.
- (R.2.2) Investigate the DSL in NIPI structures of IV–VI, II–VI and stressed Kane type compounds in the presence of an arbitrarily oriented non-quantizing magnetic field by including the electron spin.
- (R.2.3) Investigate the DSL for NIPI structures of all the materials as stated in R.1.1 of [Chap. 1](#).
- (R.2.4) Investigate the DSL for all the problems from R.2.1 to R.2.3 in the presence of an additional arbitrarily oriented electric field.
- (R.2.5) Investigate the DSL for all the problems from R.2.1 to R.2.3 in the presence of arbitrarily oriented crossed electric and magnetic fields.
- (R.2.6) Investigate the DSL for NIPI structures of the heavily-doped semiconductors in the presences of Gaussian, exponential, Kane, Halperian, Lax and Bonch-Burevich types of Band tails for all systems whose unperturbed carrier energy spectra are defined in R1.1 and R1.2 respectively.

- (R.2.7) Investigate the DSL for NIPI structures of the negative refractive index, organic, magnetic and other advanced optical materials in the presence of an arbitrarily oriented alternating electric field.
- (R.2.8) Investigate the DSL for all the NIPI systems of this chapter in the presence of finite potential wells.
- (R.2.9) Investigate the DSL for all the NIPI systems of this chapter in the presence of parabolic potential wells.
- (R.2.10) Investigate all the appropriate problems of this chapter by including the many body, image force, broadening and hot carrier effects respectively.
- (R.2.11) Investigate all the appropriate problems of this chapter by removing all the mathematical approximations and establishing the respective appropriate uniqueness conditions.

References

1. G.H. Doheler, Phys. Script. **24**, 430 (1981)
2. S. Mukherjee, S.N. Mitra, P.K. Bose, A.R. Ghatak, A. Neoigi, J.P. Banerjee, A. Sinha, M. Pal, S. Bhattacharya, K.P. Ghatak, J. Compu, Theor. Nanosc. **4**, 550 (2007)

Debye Screening Length

Effects of Nanostructured Materials

Ghatak, K.P.; Bhattacharya, S.

2014, XXXIII, 385 p. 123 illus., Hardcover

ISBN: 978-3-319-01338-1